

Development of an Automated High Throughput LCP-FRAP Assay to Guide Membrane Protein Crystallization in Lipid Mesophases

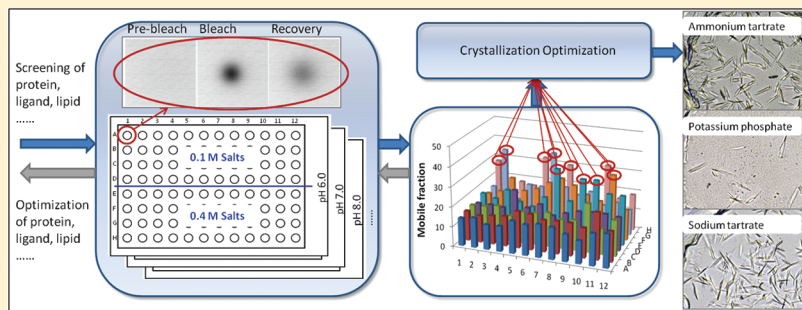
Published as part of the *Crystal Growth & Design* virtual special issue on the 13th International Conference on the Crystallization of Biological Macromolecules (ICCBM13).

Fei Xu,[#] Wei Liu,[#] Michael A. Hanson,[†] Raymond C. Stevens, and Vadim Cherezov*

Department of Molecular Biology, The Scripps Research Institute, 10550 North Torrey Pines Road, La Jolla, California 92037, United States

 Supporting Information

ABSTRACT:



Crystallization in lipidic mesophases (in meso) has been successfully used to obtain a number of high-resolution membrane protein structures including challenging members of the human G protein-coupled receptor (GPCR) family. Crystallogenesis in arguably the most successful mesophase, lipidic cubic phase (LCP), critically depends on the ability of protein to diffuse in the LCP matrix and to form specific protein–protein contacts to support crystal nucleation and growth. The ability of an integral membrane protein to diffuse in LCP is strongly affected by the protein aggregation state, the structural parameters of LCP, and the chemical environment. In order to satisfy both requirements of diffusion and specific interactions, one must balance multiple parameters, such as identity of LCP host lipid, composition of precipitant solution, identity of ligand, and protein modifications. Screening within such multidimensional crystallization space presents a significant bottleneck in obtaining initial crystal leads. To reduce this combinatorial challenge, we developed a precrystallization screening assay to measure the diffusion characteristics of a protein target in LCP. Utilizing the fluorescence recovery after photobleaching (FRAP) technique in an automated and high throughput manner, we were able to map conditions that support adequate diffusion in LCP using a minimal amount of protein. Data collection and processing protocols were validated using two model GPCR targets: the β_2 -adrenergic receptor and the A_{2A} adenosine receptor.

1. INTRODUCTION

Membrane proteins perform variety of essential functions in cell biology, such as ion and nutrient transport, signal transduction, energy conversion, and enzymatic catalysis. Malfunctions of membrane proteins in humans often lead to serious disorders and health issues. Moreover, these proteins are frequently exploited by pathogenic organisms to facilitate cell entry. Despite the significance of membrane proteins to cell physiology and human health, a fundamental understanding of structure–function relationships in this class of proteins is lagging behind their soluble counterparts in the proteome.¹ The primary reason for the deficit in membrane protein structural information relates to the inherent difficulty in obtaining diffraction quality crystals of amphipathic macromolecules. Crystallization in lipidic

mesophases (in meso)^{2,3} has proven to be a promising alternative to conventional crystallization techniques which occur in detergent solutions (in surfo). In meso crystallization has been used to obtain high-resolution structures of microbial rhodopsins,^{4–9} outer membrane proteins,^{10,11} photosynthetic proteins,^{12–14} and G protein-coupled receptors (GPCR).^{15–20} This technique takes advantage of a membrane-like environment to stabilize proteins and typically results in crystals with better packing and lower solvent content compared to in surfo crystallization.²¹

Obtaining initial crystal leads for membrane proteins is difficult due to the vast size and multidimensionality of the

Received: October 15, 2010

Revised: January 13, 2011

Published: February 18, 2011

crystallization space coupled with limited feedback during crystallization trials. This issue is compounded in the case of in meso crystallization, which adds extra dimensions related to composition of the host lipidic mesophase. Some proteins can be easily crystallized in many different conditions; however, more challenging targets require comprehensive screening of the crystallization and ligand space, as well as extensive protein engineering. Thus, there is a pressing need for precrystallization assays capable of reducing the number of variables through intermediate stage predictors of crystallizability. Such assays are beginning to emerge and have shown great utility in improving the odds of success for a given crystallization project.^{22,23} Previously, we introduced an lipidic cubic phase-fluorescence recovery after photobleaching (LCP-FRAP) assay to measure the mobility of membrane proteins in LCP and demonstrated that crystallization conditions for bacteriorhodopsin and β_2 -adrenergic receptor correlate well with higher mobile fractions and faster diffusion rates.²⁴ One drawback of the initial implementation of LCP-FRAP is low throughput. Because of the relatively slow diffusion of membrane proteins in LCP, recording a full FRAP curve requires 20–30 min of data collection, which initially limited the number of conditions that could practically be screened.

Here we present a modified protocol, termed high throughput LCP-FRAP (HT LCP-FRAP), which allowed measurement of the mobile fraction of a labeled protein under 96 different screening conditions within only 2 h. This represented more than an order of magnitude increase in efficiency relative to the original method and greatly improved the utility of the FRAP technique as a precrystallization assay platform. Data collection and processing procedures have been fully automated and validated using two previously characterized GPCR targets: β_2 -adrenergic receptor (β_2 AR) and A_{2A} adenosine receptor (A_{2A}AR).^{15,17} The utility of HT LCP-FRAP for guiding crystallization trials was demonstrated by obtaining novel crystal hits for these proteins.

2. EXPERIMENTAL SECTION

2.1. Protein Expression, Purification, and Labeling. Two model proteins used in this study, β_2 AR and A_{2A}AR, were engineered to increase their stability and facilitate crystallization, as described.^{15,17} Briefly, the β_2 AR construct contained a stabilizing mutation E122W,²⁵ removal of one N-linked glycosylation site through mutagenesis (N187E), a C-terminal truncation at residue 348, and replacement of the third intracellular loop (residues 231–262) by residues 2–161 of cysteine-free T4 lysozyme (C54T, C97A).²⁶ The A_{2A}AR construct contained a C-terminal truncation at residue 316 and T4 lysozyme fusion (replacing residues 208–221 with residues 2–161 of cysteine-free T4 lysozyme). Both constructs contained an N-terminal FLAG tag and a C-terminal 6xHis tag (β_2 AR) or 10xHis tag (A_{2A}AR) for identification and affinity purification purposes, respectively. Both proteins were expressed in *Spodoptera frugiperda* (Sf9) insect cells using a modified Bac-to-Bac expression system^{16,17} (Invitrogen) and the purification was adapted from published protocols.^{15,17} After extensive membrane washes, the purified membranes were treated with 2 mg/mL iodoacetamide (Sigma) in the presence of ligand: 1 mM timolol for β_2 AR and 4 mM theophylline for A_{2A}AR, and protease inhibitor cocktail (Roche). The target proteins were solubilized from the membranes with 0.5% w/v n-dodecyl- β -D-maltopyranoside (DDM, Anatrace), 0.1% w/v cholestryl hemisuccinate (CHS, Sigma), 50 mM HEPES pH 7.5, and 150 mM (β_2 AR) or 800 mM (A_{2A}AR) NaCl. Unsolubilized material was removed by centrifugation at 150000g for 45 min, and the clear

supernatant was incubated with TALON IMAC resin (Clontech) overnight at 4 °C.

Both proteins were labeled with Cy3-mono NHS ester (GE healthcare). This fluorophore was selected for its good solubility, the low environmental dependence of its fluorescence properties, and its relatively good stability under ambient light during sample preparation, while still being easily bleachable by laser. The pH of the buffer system used for labeling was adjusted to 7.2 to preferentially label the N-terminal amino group instead of the primary amino group of the receptor lysine residues, thereby minimizing modifications to the protein core. Adventitious labeling of free-amine containing lipids copurified with the proteins may occur when using an amino-reactive dye and result in elevated background signals from lipid diffusion in the FRAP assay.²⁴ Methods to correct this effect are discussed in Results and Discussion.

Protein labeling was performed by adding 5–10 μ L of 5 mg/mL Cy3-mono NHS ester stock in DMF (Sigma) to ~500 μ g of protein bound to 1 mL of TALON resin in 5 mL of buffer at pH 7.2. After incubation for 3 h at 4 °C in the dark, unreacted dye was removed by extensive washes using a gravity column (Bio-Rad). The wash buffer (0.1% w/v DDM, 0.02% w/v CHS, 50 mM HEPES pH 7.5, 150 mM (β_2 AR) or 800 mM (A_{2A}AR) NaCl, 10% v/v glycerol (A_{2A}AR only) and 8 mM ATP (Sigma)) contained high-affinity ligand to be exchanged for the LCP-FRAP assay: 50 μ M carazolol (β_2 AR inverse agonist) for β_2 AR, and 100 μ M ZM241385 (A_{2A}AR antagonist) or 100 μ M LUF5833 (A_{2A}AR agonist)²⁷ for A_{2A}AR. Target proteins were eluted using 5 column volumes of wash buffer with an increased imidazole concentration of 200 mM. After desalting the purified receptor to reduce the imidazole concentration, proteins were incubated with 100 μ L of Ni IMAC (GE healthcare) resin for 6 h to overnight in the presence of PNGase F (NEB) to deglycosylate the protein. PNGase F and remaining impurities were removed using 10–15 column volumes of wash buffer (0.05% w/v DDM, 0.01% w/v CHS, 50 mM HEPES pH 7.5, 150 mM (β_2 AR) or 800 mM (A_{2A}AR) NaCl, 10% v/v glycerol (A_{2A}AR only), 50 mM imidazole and ligand of interest). Receptors were subsequently eluted in a minimal volume of the same buffer supplemented with 200 mM imidazole. β_2 AR/carazolol was concentrated to 20 mg/mL in a 100 kDa cutoff concentrator (Vivascience) and immediately used for LCP-FRAP sample preparation. A_{2A}AR/ZM241385 and A_{2A}AR/LUF5833 were concentrated to 20 mg/mL, flash-frozen in liquid nitrogen, and stored in –80 °C until further use. All protein samples were evaluated for purity, monodispersity, and labeling efficiency by analytical size-exclusion chromatography (aSEC) prior to LCP-FRAP sample preparation. In the case of all receptor samples studied here, the aSEC results indicated a single monomer peak and a typical protein labeling ratio of 0.1–0.5%.

2.2. LCP-FRAP Sample Preparation. Labeled protein was reconstituted in LCP by mixing protein solution with molten monoolein (Nu Chek Prep) in a 2/3 v/v ratio using a mechanical syringe mixer.^{28–30} LCP-FRAP samples were prepared in 96-well glass sandwich plates (Paul Marienfeld GmbH, Germany) with 60 μ m thick spacers (3 M 9492MP) using an in meso crystallization robot^{29,31} by delivering 50 nL boluses of the protein-laden LCP and overlaying them with 0.8 μ L of screening solutions. After setting up and sealing wells with a glass coverslip, plates were wrapped with foil and incubated at 20 °C overnight (~12 h) to equilibrate LCP drops with screening solutions before conducting FRAP measurements.

2.3. LCP-FRAP Protocols. **2.3.1. Instrument Setup.** All FRAP experiments were performed using a custom-built LCP-FRAP station consisting of a Zeiss AxioImager A1 fluorescent microscope with HBO 100 epi-illumination and 5 \times , 10 \times , 20 \times , and 40 \times objectives; fluorescence filter sets for Bimane, Fluorescein, Rhodamine 6G and Cy3 dyes; a Micropoint dye cell laser with tunable wavelength and an adjustable microscope attachment (Photonic Instruments); a cooled (–30 °C)

CCD (1392×1040 pixels, $6.45\text{ }\mu\text{m}/\text{pixel}$) 14 bit monochrome Fire-Wire camera CoolSnap HQ2 (Photometrics); an automated XYZ microscope stage MS-2000 (Applied Scientific Instrumentation); an automatic shutter and a filter wheel with an Optiscan II controller (Prior). The hardware was controlled from a computer by the ImagePro Advanced Microscopy Suite (Media Cybernetics).

2.3.2. High Throughput LCP-FRAP Data Collection and Analysis. HT LCP-FRAP data acquisition and image analysis were fully automated using the programming capabilities of the ImagePro software. A typical procedure consisted of the following steps. (1) Drop location: The sample plate was mounted on the XYZ stage and the microscope was manually focused on the well A1. The plate was then scanned using the $5\times$ objective to determine locations and shapes of all LCP drops, which were approximated as ellipses. (2) Focusing step: The objective was switched to $10\times$, and an automatic focusing was performed for six wells: A1, A6, A12, H12, H7, and H1. At each of these wells initial crude focusing by maximizing contrast at a sample edge was followed by bleaching a spot in the sample and performing a fine focusing on the bleached spot. Z-height values for the rest of the wells were obtained by interpolation. A six-point focusing was implemented instead of a three-point in order to increase the accuracy and to account for small-scale warping in the sample plate. Typical focusing accuracy achieved by this procedure was within $10\text{--}20\text{ }\mu\text{m}$. (3) Bleaching step: Each sample was bleached sequentially at a user-defined location (typically $\sim 100\text{ }\mu\text{m}$ from the LCP drop edge) by firing $15\text{--}20$ laser pulses at a 25 Hz pulse rate. Fluorescence images before and immediately after bleaching were recorded and saved for further analysis. (4) Recovery step: After a user-defined incubation time (an adjustable parameter, typically 30 min after bleaching the first sample) the plate was scanned to record the end-state fluorescence recovery images for each sample. (5) HT LCP-FRAP data processing step: Recorded images were processed automatically to locate the bleached spot and to integrate the intensity within the spot before bleaching, immediately after bleaching and after recovery. The integrated intensities were corrected for nonlaser induced photobleaching and fluctuations of the illuminating light by normalizing to the average intensity of four reference spots selected at least $50\text{ }\mu\text{m}$ away from the laser bleached spot. The mobile fraction, M , was calculated as follows:

$$M = (I_{\text{recov}} - I_{\text{bleach}})/(I_{\text{pre-bleach}} - I_{\text{bleach}}) \quad (1)$$

Typically, the whole HT LCP-FRAP data collection and analysis procedure required approximately 2 h per 96-well plate.

2.4. Full LCP-FRAP Data Collection and Analysis. Full time-course fluorescence recovery data were collected on selected samples to characterize the protein diffusion properties in more detail. Data acquisition and analysis of the full LCP-FRAP curves were performed as previously described.²⁴ Fluorescence recovery curves after correction and normalization were fit with one or two component diffusion to obtain the mobile fraction, M , and the characteristic diffusion time, T , of the labeled molecules. The two component diffusion equation was used to obtain diffusion parameters for the slow moving proteins in the presence of fast diffusing lipids. The one component equation was used when no protein diffusion was detected. The radius of the bleached spot, R , was determined by fitting the radially integrated intensity of the bleached spot by a Gaussian. The diffusion coefficient, D , was calculated as $D = R^2/4T$.

All nonlinear curve fittings were accomplished using Prism (GraphPad Software).

2.5. Using Thin Layer Chromatography To Determine Detergent Concentrations in Protein Samples. Detergent concentration in protein solution was measured by thin-layer chromatography (TLC).³² A $10\text{ cm} \times 10\text{ cm}$ high performance thin-layer chromatography plate (HPTLC Silica gel, EMD Chemicals Inc.) was used to separate detergents (DDM and CHS) from protein and other

solution components present in protein samples. The TLC plate was prerun in solvent (chloroform/methanol/water, 65:25:4, v/v/v) to remove contaminants and impurities. After drying, $1\text{ }\mu\text{L}$ each of the following were spotted 1 cm above the bottom of the plate: detergent standards of various concentration (5%, 2%, 1%, 0.2%, 0.05% w/v DDM), elution buffer, and protein samples. The loaded TLC plate was then inserted into a closed vessel containing solvent, and chromatography was conducted until the solvent front reached approximately 1 in. from the top of the plate. The plate was then air-dried and spots were visualized by staining with iodine vapor.

3. RESULTS AND DISCUSSION

3.1. Development of HT LCP-FRAP Data Collection Protocol. The original idea behind development of a precrystallization assay measuring protein mobility in LCP was based on a presupposition that a sufficient long-range translational diffusion of protein molecules is required in order to induce crystal nucleation and maintain crystal growth. Unlike in aqueous solutions, where protein molecules of any size undergo Brownian motions, translational diffusion of large proteins or protein oligomeric aggregates embedded in lipid bilayer of LCP is restricted. A fast nonspecific aggregation of protein molecules, which is equivalent to a heavy precipitation in aqueous solutions, is not visually observable in LCP because of the limitation on the size of protein aggregates that can move through the narrow passages of LCP. The spatial constraints of the LCP effectively restrict the size of protein aggregates well below 100 nm , preventing their detection by light microscopy. Previously, we have shown that protein mobility in LCP strongly depends on the particular protein construct as well as on the composition of screening solutions equilibrated with LCP, and furthermore, that crystallization conditions correlate well with conditions supporting higher mobile fractions and faster diffusion rates of protein molecules.²⁴ These results prompted us to develop an assay for screening a range of precipitants, in order to eliminate conditions nonconducive to protein diffusion from subsequent crystallization trials, thus increasing the chance of obtaining initial crystal hits. However, since recording full recovery curves for a large number of samples was time-consuming and impractical, we modified the protocol so that only initial and final recovered states are measured, allowing for a parallel-processing of up to 96 samples. The new protocol consisted of taking a prebleached image, bleaching a spot, and recording a postbleached image for each sample in a 96-well plate sequentially. Then after an incubation of typically 30 min , images of a recovered state were taken for each sample. The procedure, which also included drop locations and focusing steps, as well as data processing was fully automated and allowed obtaining mobile fractions from 96 samples within about 2 h .

3.2. Design of Screens. As opposed to a limited readout associated with standard crystallization trials, the HT LCP-FRAP assay provided a spectrum of values for protein diffusion parameters, which were not highly sensitive to exact concentrations of screening components. Therefore, the aim behind designing screens for HT LCP-FRAP was to test a variety of precipitants at a few concentration levels and then to utilize the diffusion readout to determine the optimal range for crystallization.

Practically, the initial screens for HT LCP-FRAP were created either randomly from a range of common precipitants or more rationally using previous knowledge about the protein. In this work, we took advantage of the knowledge that crystallization

conditions for all previously obtained structures of GPCRs with fused T4L lysozyme (T4L) were composed of a buffer, PEG 400 and a salt.^{15,17,18,20,24} We decided to maintain the PEG 400 concentration constant at 30%v/v, since the primary effect of PEG 400 is to swell the LCP matrix and allow for better diffusion of the bulky T4L-fused receptors,¹⁰ and focus on exploring different pH values and salts. Therefore, a series of 96-well screens were made, each at different pH values (6, 7, and 8 for β_2 AR and 6, 7 for A_{2A}AR), containing 100 mM buffer, 30%v/v PEG 400, and 48 different salts from the Salt Stock Option kit (Hampton Research; sodium fluoride was removed and succinic acid was replaced with tacsimate pH 7.0) at two concentrations: 0.1 M (rows A–D) and 0.4 M (rows E–H), and a receptor ligand of interest.

3.3. Validation of HT LCP-FRAP Protocol. In order to assess the reliability and consistency of the HT LCP-FRAP assay, we

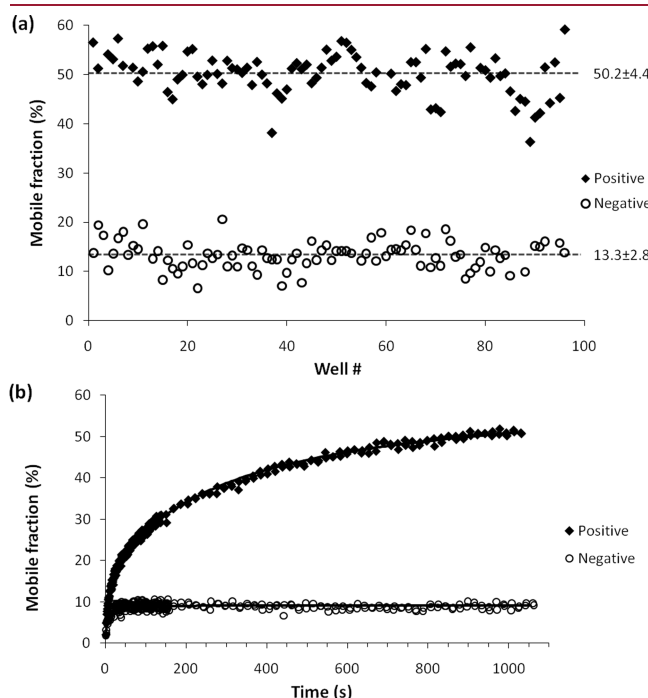


Figure 1. Validation of HT LCP-FRAP and full LCP-FRAP protocols. (a) Fluorescence recovery data obtained for β_2 AR in 96 identical positive control conditions (0.1 M HEPES pH 7.5, 30%v/v PEG 400, 0.2 M Na citrate) and 96 identical negative control conditions (0.5 M NaCl). Data were collected following the HT LCP-FRAP protocol. (b) Time-course fluorescence recovery curve recorded from individual positive and negative control wells.

selected one condition maintaining good diffusion of β_2 AR/carazolol in LCP: 0.1 M HEPES pH 7.5, 30%v/v PEG 400, and 0.2 M sodium citrate (positive control), and one condition completely abolishing long-range translational protein diffusion: 0.5 M NaCl (negative control). Two sample plates containing each of these conditions repeated 96 times were run through the automated HT LCP-FRAP data collection and processing (Figure 1a and Table 1). The obtained mobile fractions were very consistent throughout the sets with the average of $50.2 \pm 4.4\%$ for the positive control and $13.3 \pm 2.8\%$ for the negative control. Three more plates with positive controls were prepared and measured by HT LCP-FRAP, using the same protein stock but independently prepared LCP samples. Results indicated a good reproducibility between plates, with the average mobile fractions of $51.7 \pm 4.9\%$, $49.4 \pm 4.5\%$, and $50.5 \pm 5.0\%$ for the three experiments. The negative control samples produced about 10% recovery, all of which can be attributed to fast moving molecules (see Figure 1b), most likely representing labeled lipids copurified with the protein, as previously demonstrated.²⁴ Once reliably determined, this negative-control number can be subtracted from recovery data obtained at different conditions to correct for diffusion of nonprotein molecules. It should be noted, however, that due to variations in protein purification from batch to batch, and in particular with different protein constructs, the lipid content may vary substantially resulting in different levels of diffusion background. It is recommended to set up positive and negative control experiments for each new protein batch to define the baseline before testing different screening conditions. In this example, we used 0.5 M NaCl as a negative control, which shrank the LCP water channel diameter^{33,34} thereby restricting the motion of the T4L-fused receptors. For other proteins, different conditions able to serve as negative controls may be required. Possible venues for disrupting protein mobility in LCP include using buffers with a pH range outside of protein stability, destabilizing protein by depleting ligand, or denaturing protein by heating protein-laden LCP to 80 °C before setting up the sample plate.²³

3.4. Effects of Protein and Detergent Concentration. Typically, crystallization trials are performed at a protein concentration of 10–20 mg/mL.^{5,11,13} Diffraction quality crystals for structure determination of GPCRs are obtained using protein concentrations as high as 50–70 mg/mL.^{15,17,18,20} High protein concentration affects protein–protein interactions and thus as a result may affect protein diffusion in LCP. For precrystallization assays, however, it is desirable to reduce protein concentration to minimize consumption of the valuable sample. Therefore, we decided to test the effect of protein concentration on the mobile fraction measured by HT LCP-FRAP using A_{2A}AR/ZM241385

Table 1. Validation of HT-FRAP Protocol for Different Protein Samples

protein target	protein concentration (mg/mL)	detergent concentration (w/v DDM) (%)	time point (day)	averaged mobile fraction (%) ^a	
				positive control	negative control
β_2 AR/carazolol	20	0.5	1	50.2 ± 4.4	13.3 ± 2.8
A _{2A} AR/ZM241385	50	2	1	55.5 ± 6.3	22.8 ± 4.4
A _{2A} AR/ZM241385	1	0.1	1	46.4 ± 4.2	19.7 ± 3.6
A _{2A} AR/ZM241385	1	2	1	58.9 ± 4.0	21.0 ± 3.6
A _{2A} AR/ZM241385	1	2	4	49.9 ± 3.2	20.6 ± 3.8
A _{2A} AR/LUF5833	1	2	1	35.7 ± 4.3	14.5 ± 3.2

^a The averaged values represent mean \pm SD (standard deviation) of data from 96 samples (β_2 AR/carazolol) or 48 samples (all A_{2A}AR data).

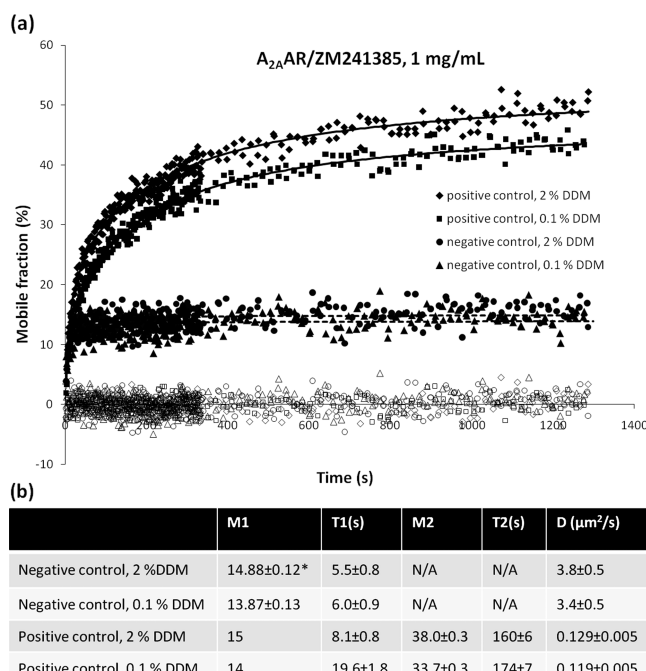


Figure 2. An example of a full LCP-FRAP curve data fitting. (a) Full LCP-FRAP curves recorded for $A_{2A}AR/ZM241385$ in positive control (0.1 M MES pH 6.0, 30%v/v PEG 400, 0.4 M Na malonate, 50 μ M ZM241385) and negative control (0.8 M NaCl) conditions at different detergent concentrations. Solid and dashed lines represent results of nonlinear curve fitting for positive and negative control data respectively. Open symbols are residuals of corresponding fits. Data fitting and calculations of residuals were performed using GraphPad. (b) Fitting results and calculations of lipid and protein diffusion rates. One component FRAP equation was used for fitting data obtained in negative control conditions accounting for diffusion of labeled lipids. Two component FRAP equation was used for fitting the recovery curves corresponding to the positive control conditions by fixing the lipid mobile fractions to values obtained from the negative control data. The diffusion coefficients were calculated as $D = R^2/4T$, where the radius of the bleached spot $R = 9.1 \mu\text{m}$. M1: the mobile fraction for lipids. T1: the characteristic diffusion time for lipids. M2: the mobile fraction for protein. T2: the characteristic diffusion time for protein. *The values represent mean \pm SEM (standard error of the mean) from nonlinear curve fitting statistics.

at 1 and 50 mg/mL. Since detergent concentrates with the protein, to evaluate the effect of detergent concentration independent of the protein concentration, in addition to the 50 mg/mL protein sample, we prepared two 1 mg/mL samples at 0.1%w/v DDM (2-fold as used during protein purification) and at 2%w/v DDM (equivalent to DDM concentration in 50 mg/mL protein sample). All three samples were screened by HT LCP-FRAP against positive (0.1 M MES pH 6.0, 30%v/v PEG 400, 0.4 M sodium malonate, 50 μ M ZM241385) and negative (0.8 M NaCl) controls, each measured 48 times in a 96-well plate (Table 1). Although the effect of protein concentration on mobile fraction was found to be negligible, elevated detergent concentration increased the mobile fraction of protein by about 10%. This behavior is in accordance with the swelling effect that detergent exerts on LCP,^{35,36} which results in decreased lipid curvature and an increase in the water channel diameter, thus relieving constraints on diffusion and inducing a higher protein mobile fraction.

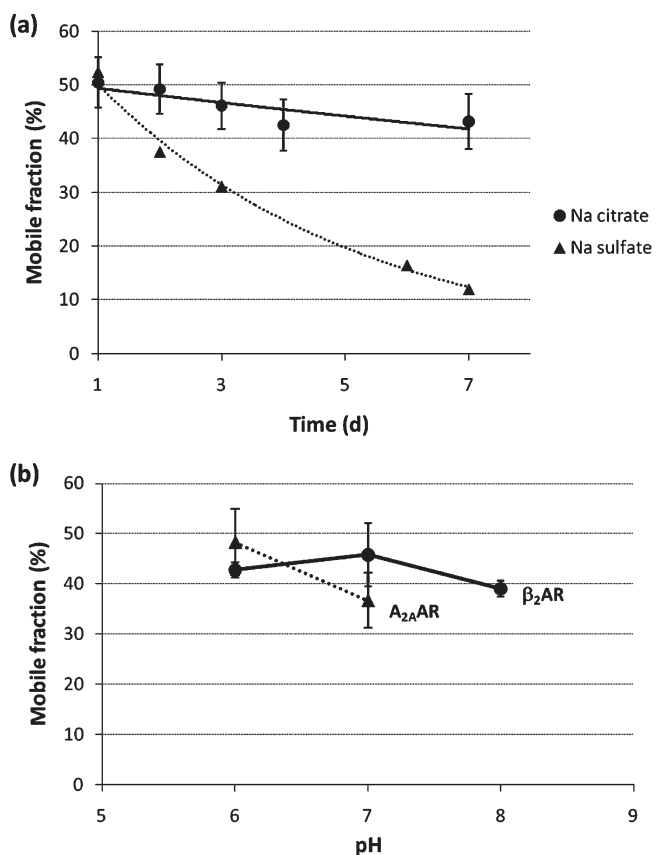


Figure 3. Dependencies of the protein mobile fraction on incubation time and pH. (a) Time-dependency of β_2 AR diffusion and stability in LCP. Fluorescence recovery was measured for the same drops at several time points within one week. The protein mobile fraction slowly decreased over one week in Na citrate condition (circles) and quickly decreased until it completely stopped in Na sulfate condition (triangles). (b) pH effect on protein mobility for β_2 AR (circles) and $A_{2A}AR$ (triangles). In both cases, the averaged mobile fraction from the four best salts inducing high protein mobility was calculated and compared at different pHs.

The HT LCP-FRAP protocol provided only total recovered fraction in a bleached spot after a certain incubation time. However, a full analysis of the diffusion properties of protein molecules can be performed by recording a complete recovery curve. Data acquisition and processing of full LCP-FRAP curves have been automated. Full recovery curves can be fitted with one (lipid only) or two (lipid and protein) component diffusion equations to obtain mobile fractions and diffusion rates of each component.²⁴ Fitting with the two component diffusion was more robust when at least one of the parameters was fixed, such as the mobile fraction of lipids, which could be obtained from the negative control measurements. Full LCP-FRAP data for two 1 mg/mL $A_{2A}AR/ZM241385$ samples at 0.1% and 2%w/v DDM concentrations and their fits are shown in Figure 2. Consistent with the HT LCP-FRAP results, the sample containing 2%w/v DDM gave a slightly higher protein mobile fraction but virtually the same diffusion rates.

On the basis of these experiments, we concluded that HT LCP-FRAP assays can be performed at a protein concentration of as low as 1 mg/mL, in which the detergent content could optionally be adjusted to better mimic conditions achieved during crystallization trials. According to our observations, even

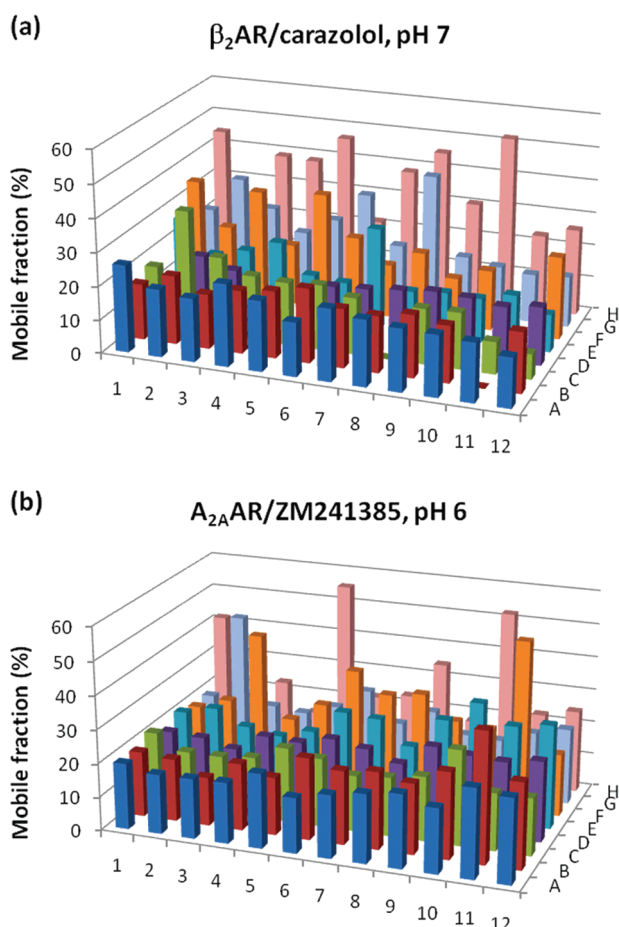


Figure 4. HT LCP-FRAP experiments for β_2 AR/carazolol and A_{2A} AR/ZM241385. (a) Fluorescence recovery for β_2 AR/carazolol in Tris pH 7 plate containing 96 salt conditions. (b) Fluorescence recovery for A_{2A} AR/ZM241385 in MES pH 6 plate. In each plate, 48 different salts from Salt Stock Option kit (Hampton Research) were arranged from A1 to D12 and E1 to H12 in a 96-well plate. Salt concentrations in rows A–D are 0.1 M, E–H are 0.4 M. Experiments were repeated at least four times for each screening plate and the averaged data was used to generate this plot.

without adjusting the detergent concentration, the HT LCP-FRAP assay performed at 1 mg/mL protein concentration captures the same trends as the assay performed at protein concentrations used in crystallization trials. It is possible, however, that other membrane proteins display stronger dependency of diffusion on concentration than those that we studied in this work. In order to save valuable protein material, our recommendation is to conduct initial assays at \sim 1 mg/mL protein concentration. When suitable conditions supporting high protein mobility are found, the assays at these conditions can be repeated at the protein concentration used in crystallization trials (10–50 mg/mL) to verify dependence of protein diffusion on concentration.

3.5. Protein Stability in LCP. Protein stability and its ability to diffuse in LCP are related to each other. Destabilized proteins usually unfold or aggregate, which results in loss of their mobility. Another reason for a decrease in mobile fraction is depletion of mobile protein consumed by crystal growth. Thus, monitoring protein mobile fractions over a period of time at different conditions by HT LCP-FRAP provided insights into protein stability and gave indications of how long one can expect crystal

growth to continue. Two conditions resulting in high initial mobile fractions for β_2 AR/carazolol were selected for these experiments and have been followed by HT LCP-FRAP over the course of 7 days (Figure 3a). Decay of the mobile fraction over time was fit to an exponential function, giving a characteristic decay time of 4.3 days for the condition containing sodium sulfate and 36 days for the condition containing sodium citrate. Initial crystals leading to the first structure of β_2 AR/carazolol were obtained in the presence of sodium sulfate. It is interesting to note, however, that although the HT LCP-FRAP experiments were performed at a sodium sulfate concentration (0.4 M) outside of the concentration range inducing crystal growth (0.1–0.3 M) and consequently no crystals were observed in the samples, the time frame during which β_2 AR/carazolol remains mobile coincides with the time frame of crystal growth (up to 6 days). This means that the short time window for crystal growth can be explained by relatively low protein stability with respect to aggregation in the presence of sodium sulfate. On the other hand, sodium citrate keeps the protein in a mobile state for a much longer time, suggesting that adding it to crystallization screens may improve crystal growth, which was explored in the case of A_{2A} AR-T4L/LUF5833 as explained later.

3.6. Effects of Precipitant Screens. *3.6.1. Effect of Salts.* After establishing and validating the HT LCP-FRAP protocol, we assayed samples of β_2 AR/carazolol and A_{2A} AR/ZM241385 in LCP against a set of 96-well screens described in section 3.2. Typical results are shown in Figure 4. Mobile fractions ranged from 8 to 52% for β_2 AR and 14 to 55% for A_{2A} AR depending on salt identity and concentration. The fraction of labeled lipid, as determined from negative control samples was 13% for β_2 AR and 20% for A_{2A} AR. Accordingly, we set a threshold level 15% above the lipid background to evaluate the effect of different salts. Among 48 salts, 15 (β_2 AR) and 9 (A_{2A} AR) salts maintained mobile fractions above the threshold level. For β_2 AR these salts are ammonium phosphate, lithium acetate, lithium citrate, lithium sulfate, potassium citrate, potassium phosphate, potassium/sodium tartrate, sodium citrate, sodium formate, sodium phosphate, sodium malonate, sodium sulfate, sodium tartrate, sodium thiocyanate, and tacsimate (a collection of organic salts, pH 7, Hampton Research). For A_{2A} AR, the best salts are ammonium tartrate, lithium citrate, magnesium acetate, nickel chloride, potassium citrate, sodium citrate, sodium malonate, sodium tartrate, and tacsimate.

Analysis of these data revealed a dominance of organic salts with monovalent cations for both proteins used in this study, as well as sulfate and phosphate anions in the case of β_2 AR. Small organic acids have been previously praised for their success in stabilization and crystallization of macromolecules.³⁷ Monovalent cations have been shown to play a role as allosteric modulators in A_{2A} AR.³⁸ Finally, sulfate was used for crystallization of β_2 AR/carazolol and A_{2A} AR/ZM241385 in LCP, and many sulfate ions are observed in crystallographic structures of both proteins.^{15,17}

Most salts promoted better diffusion at higher concentration; however, there were a few exceptions where a higher protein mobile fraction was observed at 0.1 M salt concentration (see Supporting Information, Supplementary Figure 1 for details).

3.6.2. Effect of pH. Comparative analysis of HT LCP-FRAP data obtained at different pH levels revealed that within the tested range the effect of pH on diffusion behavior of β_2 AR or A_{2A} AR is minimal; pointing to the same sets of salts that induce protein mobility regardless of pH. To quantify the effect of pH,

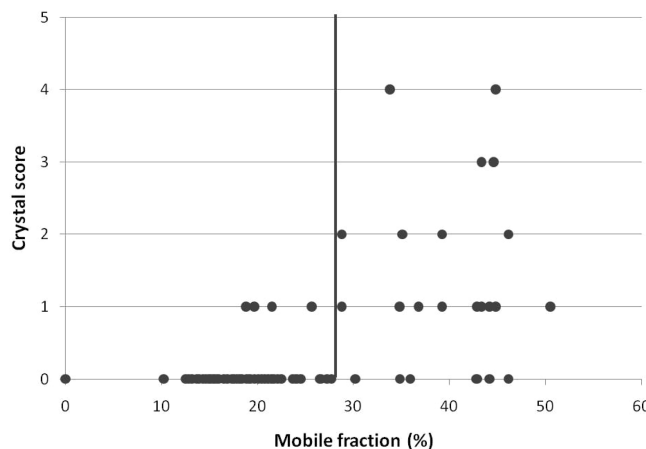


Figure 5. Correlation between mobile fraction and crystal hits for β_2 AR/carazolol. Crystal hits observed from HT LCP-FRAP experiments (Tris pH 8 plate) were scored according to crystal quality (0 - no crystals, 1 - showers of tiny crystals $<1\ \mu\text{m}$, 2 - microcrystals (between 1 and $5\ \mu\text{m}$), 3 - microcrystals (between 5 and $10\ \mu\text{m}$), and 4 - relatively large crystals $>10\ \mu\text{m}$). Crystal scores were plotted as a function of protein mobile fraction in corresponding screen conditions.

we calculated the average mobile fractions produced by the four best salts at each tested pH for β_2 AR or A_{2A} AR and plotted them in Figure 3b. The plot suggested a small trend of better mobility for β_2 AR at pH 6 and 7 as compared to pH 8, consistent with observations of better crystals obtained at pH between 6.5 and 7.^{15,16} Further, a more pronounced effect for A_{2A} AR was seen, revealing a difference of about 10% between mobile fractions obtained at pH 6 and 7, which is consistent with previous knowledge that lower pH has a stabilizing effect on A_{2A} AR.¹⁷ We emphasize that the choice of tested pH range in our experiments was based on known crystallization conditions for the two well-characterized receptors, however, and that testing an expanded pH range for HT LCP-FRAP screens may be required for a novel membrane protein target or a different protein construct.

3.7. Correlation between Mobile Fraction and Crystal Hits. Initial results on the diffusion properties of β_2 AR/carazolol in LCP in the vicinity of known crystallization space indicated a strong correlation between high protein mobility and crystallization.²⁴ Development of the HT LCP-FRAP allowed screening a broader swathe of crystallization space, enabling us to extend this correlation to a broader range of salts typically used in crystallization screens. For this purpose, we set up LCP samples loaded with 20 mg/mL of Cy3 labeled β_2 AR/carazolol against pH 8 96-well screen described in section 3.2 in duplicate and collected HT LCP-FRAP data after 12 h of incubation. The same trials were imaged in the Cy3 fluorescence channel on the LCP-FRAP station using an automated imaging option integrated in the data acquisition script after 5 days of incubation to check for crystal growth. Protein labeling substantially enhanced crystal detection, as most of the crystal hits contained showers of tiny crystals invisible under brightfield illumination.^{39,40} Crystal hits were scored on a scale of 0–4, where 0 corresponds to no crystals, 1 - showers of tiny crystals $<1\ \mu\text{m}$, 2 - microcrystals (between 1 and $5\ \mu\text{m}$), 3 - microcrystals (between 5 and $10\ \mu\text{m}$), and 4 - relatively large crystals $>10\ \mu\text{m}$.

The crystal scores were plotted against the mobile fractions, and the threshold for the mobile fractions was set at 28% based on the negative control data (Figure 5). A good correlation between crystal formation and protein mobility was evident from

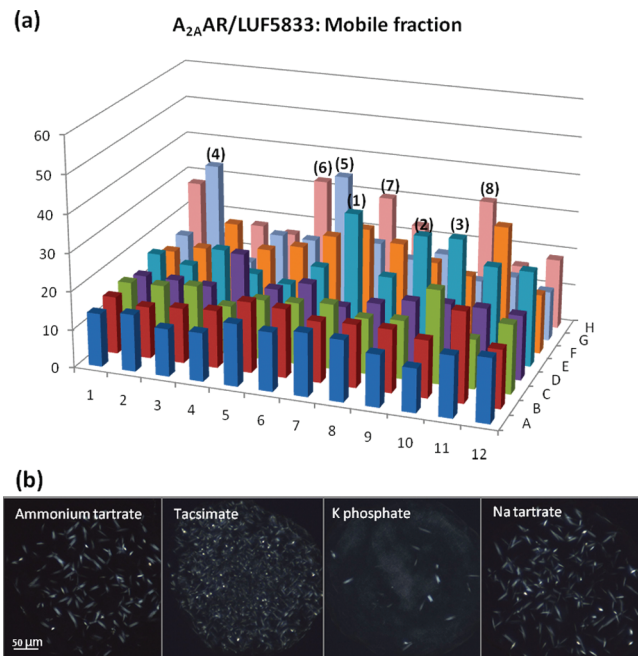


Figure 6. Mobile fractions and crystal hits for A_{2A} AR/LUF5833. (a) Results of HT LCP-FRAP experiments. The following promising salts were selected for crystallization trials: (1) ammonium phosphate, (2) ammonium sulfate, (3) ammonium tartrate, (4) K citrate, (5) K phosphate, (6) Na malonate, (7) Na sulfate, (8) tacsimate. Crystal hits were observed from screens designed by combining Na citrate pH 6 buffer with the above eight salts and combinations of promising anions and cations at a wide range of concentration gradients. (b) Examples of crystal hits obtained in ammonium tartrate, tacsimate, K phosphate, and Na tartrate. Images were taken using crossed polarizers.

the data. Protein diffusion was observed in 23 conditions (15 unique salts), while the crystals formed in 21 conditions (14 unique salts). Six conditions showed protein diffusion with no crystals, which would be expected, as good mobility alone does not guarantee crystal formation. Four conditions produced crystals but with no diffusion, perhaps, due to the rapid onset of crystallogenesis combined with the overlap of the bleaching spot with multiple microcrystalline objects which would give an artificially low value for the protein mobile fraction. Careful inspection of images taken during HT LCP-FRAP measurements to identify such events should lower the chances of rejecting promising conditions. Overall, the HT LCP-FRAP prescreening was able to enrich the success rate of these screens from 21 crystal hits of 96 conditions to 17 crystal hits of 23 conditions. Without protein labeling, however, only four conditions could be reliably identified, three of which have been previously known (lithium sulfate, sodium sulfate, sodium formate).

The same correlation profile was found for A_{2A} AR/ZM241385. Unlike the β_2 AR, the HT LCP-FRAP experiment for A_{2A} AR was carried out with low-concentration protein samples (1 mg/mL), while the crystallization trials were set up with highly concentrated protein samples (~ 50 mg/mL) using the same pH 6 HT LCP-FRAP salt screen. Among the 96 salt conditions, 14 (10 unique salts) produced crystal hits. Nine of these salts are organic (citrate, tartrate, malonate, formate), and one is sulfate. Seven of them are among the top 10 conditions with the highest mobile fraction in the corresponding HT LCP-FRAP experiment performed with 1 mg/mL protein samples, suggesting a reliable correlation.

3.8. From HT LCP-FRAP to Crystallization Hits. Given a growing number of examples demonstrating an agreement between conditions maintaining protein mobility and conditions inducing crystal nucleation and growth for model proteins, we decided to explore the ability of HT LCP-FRAP to guide crystallization trials for a more challenging target: A_{2A}AR-T4L bound to an agonist LUF5833.²⁷ Initial crystallization screening around the successful conditions for A_{2A}AR/ZM241385 did not produce any crystal hits.

First, we performed control measurements with 1 mg/mL of labeled A_{2A}AR/LUF5833 protein using the same positive and negative screens as for A_{2A}AR/ZM241385 except that LUF5833 was supplemented to the screens instead of ZM241385. Although the average mobile fraction from 48 positive screen conditions was 36% ($\pm 4\%$) (Table 1), which is 23% lower than in the case of A_{2A}AR/ZM241385, we were still able to distinguish the mobile fraction of protein molecules from the fraction caused by lipids (14.5 \pm 3.2%) in this sample. Next, with the same protein sample, we performed the HT LCP-FRAP experiment using a 96 salt screen with MES pH 6 buffer. We found 10 unique salt conditions that promoted high protein diffusion with mobile fraction above the 28% threshold (Figure 6a and Supporting Information, Supplementary Figure 1c). These salts included mostly organic salts: tartrate, citrate, malonate, and monovalent cations: ammonium, potassium, and sodium. Four of these salt conditions have been previously identified as successful crystallants for A_{2A}AR/ZM241385. However, an initial effort of searching for A_{2A}AR/LUF5833 crystal hits by grid optimization of these conditions failed, perhaps due to the more dynamic nature of A_{2A}AR bound to an agonist. Therefore, we proposed that a combination of two or more salts might be able to better modulate the protein–protein and protein–cubic phase interaction and facilitate crystallogenesis. Thus, we prepared new screens using pH 6 sodium citrate buffer instead of MES, inspired by the results that sodium citrate was one of the salts promoting protein mobility. Sixteen salts with concentrations between 40 and 400 mM were used in these screens: half of them were among the top 10 promising salt candidates (mobile fraction >28%, except for nickel chloride and sodium citrate) according to the HT LCP-FRAP results (Figure 6a), and the other half contained combinations of the most promising anions and cations. Crystallization trials with these screens successfully yielded initial crystal hits for A_{2A}AR/LUF5833 (Figure 6b) in a number of salts including four that induced high protein mobility in HT LCP-FRAP assays, highlighting the great potential in using this assay for guiding crystallization trials. The initial crystals of A_{2A}AR/LUF5833 diffracted to ~ 5 Å and the crystal optimization process is currently underway. In addition, application of HT LCP-FRAP led to rapid identification of initial crystallization hits for the dopamine D3 and the CXCR4 chemokine G protein-coupled receptors, structures of which have recently been published.^{18,20}

■ ASSOCIATED CONTENT

§ Supporting Information. Bar graphs for HT LCP-FRAP experiments for β_2 AR/carazolol, A_{2A}AR/ZM241385, and A_{2A}AR/LUF5833 (Supplementary Figure 1). This material is available free of charge via the Internet at <http://pubs.acs.org>.

■ AUTHOR INFORMATION

Corresponding Author

*E-mail: vcherezo@scripps.edu.

Present Addresses

[†]Receptos, 10835 Road to the Cure, Suite 205, San Diego, CA 92121, USA.

Author Contributions

[#]These authors contributed equally.

Funding Sources

This work has been funded by the NIH grants GM073197 and 621 RR025336.

■ ACKNOWLEDGMENT

The authors thank E. Chien, K. Allin, and T. Trinh for help with protein expression, M. McCormick for careful review of the manuscript, and A. Walker for assistance with the manuscript preparation. The authors acknowledge Dr. Laura Heitman from Leiden University for the source of LUF5833 compound. The authors also acknowledge A. Kolatkar and J. Kunken for their contributions into earlier stages of LCP-FRAP development. This work has been funded by the NIH grants GM073197 and RR025336. The authors acknowledge Yuan Zheng (The Ohio State University) and Martin Caffrey (Trinity College, Dublin, Ireland) for the generous loan of the in meso robot (built with support from the National Institutes of Health [GM075915], the National Science Foundation [IIS0308078], and Science Foundation Ireland [02-IN1-B266]).

■ REFERENCES

- (1) Raman, P.; Cherezov, V.; Caffrey, M. *Cell. Mol. Life Sci.* **2006**, 63, 36–51.
- (2) Landau, E. M.; Rosenbusch, J. P. *Proc. Natl. Acad. Sci. U. S. A.* **1996**, 93, 14532–14535.
- (3) Caffrey, M. *J. Struct. Biol.* **2003**, 142, 108–132.
- (4) Pebay-Peyroula, E.; Rummel, G.; Rosenbusch, J. P.; Landau, E. M. *Science* **1997**, 277, 1676–1681.
- (5) Luecke, H.; Schobert, B.; Richter, H. T.; Cartailler, J. P.; Lanyi, J. K. *J. Mol. Biol.* **1999**, 291, 899–911.
- (6) Kolbe, M.; Besir, H.; Essen, L. O.; Oesterhelt, D. *Science* **2000**, 288, 1390–1396.
- (7) Royant, A.; Nollert, P.; Edman, K.; Neutze, R.; Landau, E. M.; Pebay-Peyroula, E.; Navarro, J. *Proc. Natl. Acad. Sci. U.S.A.* **2001**, 98, 10131–10136.
- (8) Gordeliy, V. I.; Labahn, J.; Moukhametzianov, R.; Efremov, R.; Granzin, J.; Schlesinger, R.; Buldt, G.; Savopol, T.; Scheidig, A. J.; Klare, J. P.; Engelhard, M. *Nature* **2002**, 419, 484–487.
- (9) Vogeley, L.; Sineshchekov, O. A.; Trivedi, V. D.; Sasaki, J.; Spudich, J. L.; Luecke, H. *Science* **2004**, 306, 1390–1393.
- (10) Cherezov, V.; Liu, W.; Derrick, J. P.; Luan, B.; Aksimentiev, A.; Katritch, V.; Caffrey, M. *Proteins* **2008**, 71, 24–34.
- (11) Cherezov, V.; Yamashita, E.; Liu, W.; Zhalmina, M.; Cramer, W. A.; Caffrey, M. *J. Mol. Biol.* **2006**, 364, 716–734.
- (12) Katona, G.; Andreasson, U.; Landau, E. M.; Andreasson, L. E.; Neutze, R. *J. Mol. Biol.* **2003**, 331, 681–692.
- (13) Cherezov, V.; Clogston, J.; Papiz, M. Z.; Caffrey, M. *J. Mol. Biol.* **2006**, 357, 1605–1618.
- (14) Wohri, A. B.; Wahlgren, W. Y.; Malmerberg, E.; Johansson, L. C.; Neutze, R.; Katona, G. *Biochemistry* **2009**, 48, 9831–9838.
- (15) Cherezov, V.; Rosenbaum, D. M.; Hanson, M. A.; Rasmussen, S. G.; Thian, F. S.; Kobilka, T. S.; Choi, H. J.; Kuhn, P.; Weis, W. I.; Kobilka, B. K.; Stevens, R. C. *Science* **2007**, 318, 1258–1265.
- (16) Hanson, M. A.; Cherezov, V.; Griffith, M. T.; Roth, C. B.; Jaakola, V. P.; Chien, E. Y.; Velasquez, J.; Kuhn, P.; Stevens, R. C. *Structure* **2008**, 16, 897–905.

- (17) Jaakola, V. P.; Griffith, M. T.; Hanson, M. A.; Cherezov, V.; Chien, E. Y. T.; Lane, J. R.; Ijzerman, A. P.; Stevens, R. C. *Science* **2008**, 322, 1211–1217.
- (18) Chien, E. Y.; Liu, W.; Zhao, Q.; Katritch, V.; Han, G. W.; Hanson, M. A.; Shi, L.; Newman, A. H.; Javitch, J. A.; Cherezov, V.; Stevens, R. C. *Science* **2010**, 330, 1091–1095.
- (19) Wacker, D.; Fenalti, G.; Brown, M. A.; Katritch, V.; Abagyan, R.; Cherezov, V.; Stevens, R. C. *J. Am. Chem. Soc.* **2010**, 132, 11443–11445.
- (20) Wu, B.; Chien, E. Y.; Mol, C. D.; Fenalti, G.; Liu, W.; Katritch, V.; Abagyan, R.; Brooun, A.; Wells, P.; Bi, F. C.; Hamel, D. J.; Kuhn, P.; Handel, T. M.; Cherezov, V.; Stevens, R. C. *Science* **2010**, 330, 1066–1071.
- (21) Caffrey, M. *Annu. Rev. Biophys.* **2009**, 38, 29–51.
- (22) Alexandrov, A. I.; Mileni, M.; Chien, E. Y.; Hanson, M. A.; Stevens, R. C. *Structure* **2008**, 16, 351–359.
- (23) Liu, W.; Hanson, M. A.; Stevens, R. C.; Cherezov, V. *Biophys. J.* **2010**, 98, 1539–1548.
- (24) Cherezov, V.; Liu, J.; Griffith, M.; Hanson, M. A.; Stevens, R. C. *Cryst. Growth Des.* **2008**, 8, 4307–4315.
- (25) Roth, C. B.; Hanson, M. A.; Stevens, R. C. *J. Mol. Biol.* **2008**, 376, 1305–1319.
- (26) Rosenbaum, D. M.; Cherezov, V.; Hanson, M. A.; Rasmussen, S. G. F.; Thian, F. S.; Kobilka, T. S.; Choi, H. J.; Yao, X. J.; Weis, W. I.; Stevens, R. C.; Kobilka, B. K. *Science* **2007**, 318, 1266–1273.
- (27) Beukers, M. W.; Chang, L. C.; von Frijtag Drabbe Kunzel, J. K.; Mulder-Krieger, T.; Spanjersberg, R. F.; Brussee, J.; AP, I. J. *J. Med. Chem.* **2004**, 47, 3707–3709.
- (28) Cheng, A. H.; Hummel, B.; Qiu, H.; Caffrey, M. *Chem. Phys. Lipids* **1998**, 95, 11–21.
- (29) Caffrey, M.; Cherezov, V. *Nat. Protoc.* **2009**, 4, 706–731.
- (30) Cherezov, V.; Abola, E.; Stevens, R. C. *Methods Mol. Biol.* **2010**, 654, 141–168.
- (31) Cherezov, V.; Peddi, A.; Muthusubramaniam, L.; Zheng, Y. F.; Caffrey, M. *Acta Crystallogr. D Biol. Crystallogr.* **2004**, 60, 1795–1807.
- (32) Eriks, L. R.; Mayor, J. A.; Kaplan, R. S. *Anal. Biochem.* **2003**, 323, 234–241.
- (33) Cherezov, V.; Fersi, H.; Caffrey, M. *Biophys. J.* **2001**, 81, 225–242.
- (34) Nollert, P.; Qiu, H.; Caffrey, M.; Rosenbusch, J. P.; Landau, E. M. *FEBS Lett.* **2001**, 504, 179–186.
- (35) Ai, X.; Caffrey, M. *Biophys. J.* **2000**, 79, 394–405.
- (36) Misquitta, Y.; Caffrey, M. *Biophys. J.* **2003**, 85, 3084–3096.
- (37) McPherson, A. *Protein Sci.* **2001**, 10, 418–422.
- (38) Gao, Z. G.; Ijzerman, A. P. *Biochem. Pharmacol.* **2000**, 60, 669–676.
- (39) Fry, E. H.; Qin, W.; Fleck, E. N.; Judge, R. A.; Chiu, M. L. *Open Struct. Biol. J.* **2009**, 3.
- (40) Forsythe, E.; Achari, A.; Pusey, M. L. *Acta Crystallogr. D Biol. Crystallogr.* **2006**, 62, 339–346.